

Magnetic Surface Mapping Experiments in TJ-II Heliac

ASCASÍBAR Enrique*, QIN Jiang and LÓPEZ-FRAGUAS Antonio
Asociación EURATOM-CIEMAT para Fusión, Ciemat. 28040 Madrid, Spain

(Received: 30 September 1997/Accepted: 22 October 1997)

Abstract

In December 1996 a short campaign of magnetic surface measurements were carried out in TJ-II. A limited number of configurations were studied with the main goal of checking that the high accuracy required in positioning of the coils and the vacuum vessel had been achieved. The existence of closed and nested magnetic surfaces, in good agreement with the calculated ones, demonstrated this issue. In this work the results obtained are discussed.

Keywords:

helical axis stellarator, magnetic surfaces

1. Description of the Device

The flexible Heliac TJ-II is a medium size device ($R=1.5$ m, $\langle a \rangle = 0.2$ m, $\bar{B}(0)=1.0$ T) located at CIEMAT, Madrid, and about to start plasma operation [1]. TJ-II coil configuration consists of 32 toroidal field (TF) coils centred around a four periods toroidal helix. Two additional coils provide its unique flexibility ($0.96 \leq t_0 \leq 2.5$, $-1\% \leq \text{magnetic well} \leq 6\%$), a circular coil located at the major axis, 1.5 m, and a helical winding wrapped around the circular one, following the same winding law as the toroidal coils. Two poloidal field coils (2.25 m radius) complete the coil configuration.

2. Experimental Results

First measurements of the magnetic surfaces in the device were performed in December 1996, using a directed electron beam in combination with a movable fluorescent rod array [2-6]. At that time, the final adjustment of the TF coils was still not finished, so that the maximum deviation of some of them respect to the nominal position (2.9 mm, in radial direction) exceeded the design tolerance (1 mm). The magnetic field was steady state, $B_0 \leq 0.05$ T (5% of the nominal field), with 50 s pulse length. The technique used is based on

imaging the spots produced by the impact of an electron beam, launched in the vacuum vessel along the magnetic field lines, when intersecting an array of four fluorescent rods (1.5 mm diameter each, coated with P24, ZnO:Zn powder), sketched in Fig. 1, that sweeps the vessel cross section. The electron beam (0.5 mm diameter at the gun exit; energy 150 eV) is launched with the main velocity component, v_i , parallel to the magnetic field of the device. The gun head is driven over a rectangular region (147 mm in radial direction, 328 mm in vertical direction) by means of a PLC controlled manipulator installed in a top port; the magnetic surfaces are measured about 199° away in toroidal direction. Three LEDs located inside the vacuum vessel, at the same cross-section where the image is formed, are used as a reference system for measuring distances. The images are acquired with an intensified CCD camera looking perpendicularly to the image plane through a tangential NBI port and processed by means of an image integrator. The spatial resolution of the experimental system is estimated to be about 2 mm (fluorescent rod, 1.5 mm thick, plus the space charge broadening of the electron beam cross section as it travels around the torus).

*Corresponding author's e-mail: ascasibar@ciemat.es

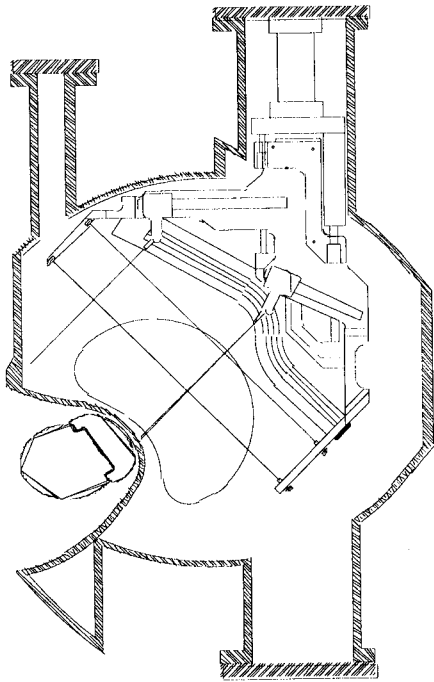


Fig. 1 Schematic view of the fluorescent detector.

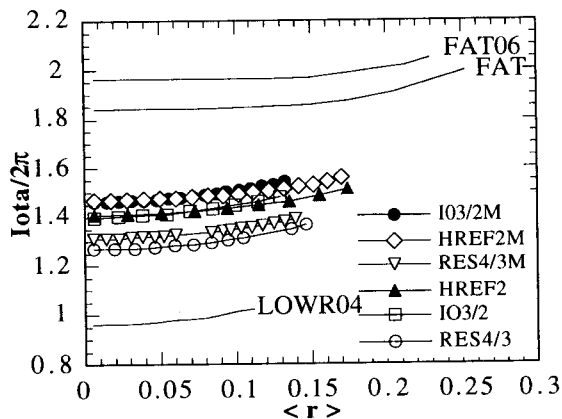


Fig. 2 Theoretical rotational transform profiles of the measured configurations.

TJ-II configurations are low shear. Nine of them have been measured, covering the iota range $0.96 \leq \iota_0 \leq 1.97$. Their iota profiles are shown in Fig. 2. In all the studied configurations closed and nested magnetic surfaces are found, provided that the low order resonances ($\iota=1, 3/2$ and 2 , in our case) are kept away from the corresponding rotational transform profile. Size and shape of the magnetic surfaces, as well as the coil current values needed for all the configurations, fully agree with the design parameters. Figure 3 shows

that the calculated and experimental surfaces for the standard configuration, named HREF2 ($\iota \leq 3/2$), are in very good agreement. If the $\iota=3/2$ value is allowed inside this low shear configuration, rather large islands are measured, see Fig. 4, probably due to the above mentioned non corrected internal field error, in good qualitative agreement with the theoretical model. The measured island size is larger than the calculated one. Calculations with a different coil modelling, having lower shear at the resonant value, $\iota=3/2$, yield larger island size, in better agreement with the experiment. However, this model is less accurate because the calculated rational ι -values are obtained for coil currents about 10% away from the measured ones. This seems to indicate that the real shear could be lower than the predicted one. After final positioning of the TF coils, within the design tolerances, additional experiments and calculations must be done to further investigate this point.

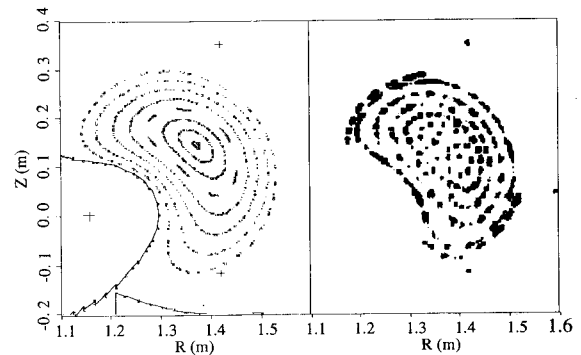


Fig. 3 Calculated and experimental surfaces for the standard (HREF2) configuration.

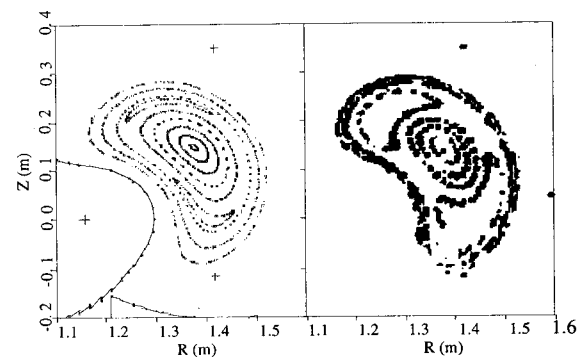


Fig. 4 Calculated and experimental surfaces for the HREF2M configuration.

The ideal vacuum field contains field components, associated with the four-fold toroidal symmetry, that lead to the appearance of natural islands on magnetic surfaces with $\iota=(n=4)/m$. This has been experimentally confirmed for the $\iota=4/3$ case, named RES4/3M, where the agreement with the theoretical model is remarkable, as shown in Fig. 5. In the experimental image only individual points are found for the two most external surfaces because the second transit of the electron beam is intercepted by the vacuum vessel, whose finite thickness is not taken into account in the calculation. It should be noted that the apparent displacement of the secondary magnetic axis of the islands, in the experimental image, is due to the finite size of the electron gun head (9 mm diameter). Figure 6 shows the good agreement between experimental and calculated magnetic surfaces corresponding to one of the configurations with largest plasma volume, named FAT (0.25 m effective plasma radius; ι ranging between 1.84 and 1.99). In the external part of the theoretical image, part

of an island corresponding to $\iota=2$ is clearly visible. It couldn't be resolved in the experiment because it would be partially intersected by the vessel wall, but, probably, this is the reason why the last experimental contour appears to be not clearly closed. In Fig. 7 another comparison between theory and experiment is presented. It corresponds to one of the smallest configurations in terms of plasma radius, named LOWRO4 (0.11 m effective plasma radius; ι ranging between 0.96 and

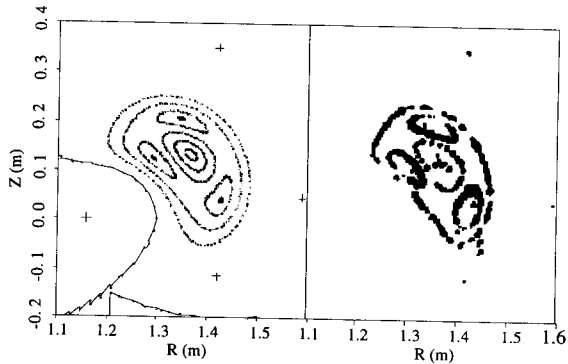


Fig. 5 Calculated and experimental surfaces for the RES4/3M configuration.

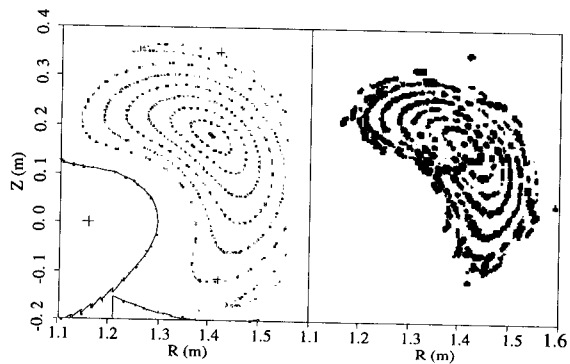


Fig. 6 Calculated and experimental surfaces for the FAT configuration.

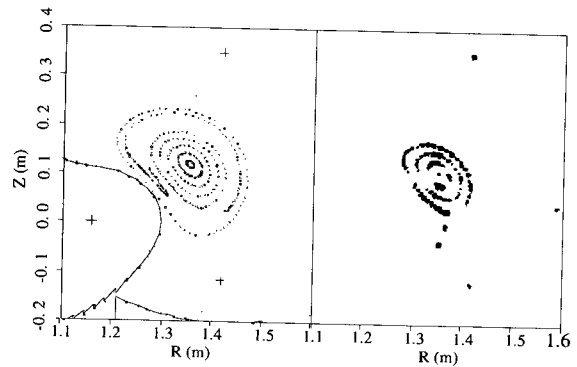


Fig. 7 Calculated and experimental surfaces for the LOWRO4 configuration.

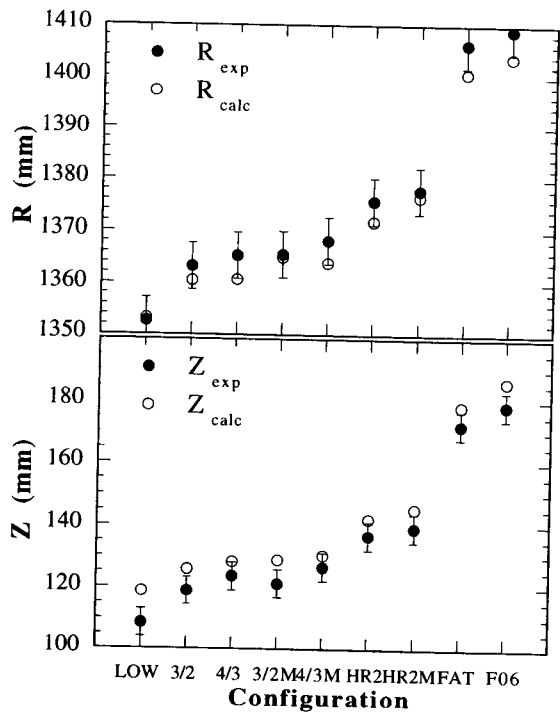


Fig. 8 Experimental and calculated values of R and Z coordinates of the magnetic axis, at the detection plane.

1.02). Again the similarity between theory and experiment is clear. In the region close to the external $\iota=1$ island only the first transit of the electron beam can be found because subsequent transits are intercepted by the electron gun head. Fig. 8 shows the comparison between experimental and calculated positions of R and Z coordinates of the magnetic axis at the detection plane, for all the measured configurations. As regards R coordinate, the agreement is quite good, but for the Z coordinate, a systematic discrepancy of 6 mm, in average, between experimental and calculated values is observed. The magnetic field in the experimental hall where TJ-II is located has been measured, yielding values of 0.5 G in vertical direction and 0.2 G in the horizontal one. So, no perturbations apart from the earth magnetic field appear to be present. This small external magnetic field does not account for the above mentioned discrepancy. Its origin is still being investigated.

Acknowledgements

The authors wish to thank the help from A. Gabriel, R. Perales and J. Agulló in designing and constructing the fluorescent detector as well as the support from A. Unamuno, L. Pallás, A. López, A. Montoro in designing and commissioning the electron gun manipulator and its control unit.

References

- [1] C. Alejaldre *et al.*, *Fusion Technol.* **17**, 131 (1990).
- [2] H. Hailer *et al.*, *Controlled Fusion and Plasma Physics (Proc. 14th Eur. Conf. Madrid, 1987)*, Vol. 11D, Part I, European Physical Society, p.423 (1987).
- [3] R. Jaenicke *et al.*, *Nucl. Fusion* **33**, 687 (1993).
- [4] G.G. Lesnyakov *et al.*, *Nucl. Fusion* **32**, 2157 (1992).
- [5] H. Lin *et al.*, *Rev. Sci. Instrum.* **66**, 464 (1995).
- [6] Shats *et al.*, *Nucl. Fusion* **34**, 1653 (1994).
- [7] E. Ascasíbar *et al.*, *Nucl. Fusion* **37**, 851 (1997).